Fluorescence properties of aromatic amine adsorbed on metallic and semiconducting single-walled carbon nanotubes

Satoshi Kubota,[a] Takafumi Maruyama,[a] Hiromasa Nishikiori,[a*] Fuyuki Ito,[b] Nobuaki Tanaka,[a] Morinobu Endo,[c] Tsuneo Fujii[a,d]

[a]Department of Environmental Science and Technology, Faculty of Engineering, Shinshu University, Wakasato, Nagano 380-8553, Japan

[b]Department of Chemistry, Faculty of Education, Shinshu University, 6-ro, Nishinagano, Nagano 380-8455, Japan

[c]Department of Electrical and Electronic Engineering, Faculty of Engineering, Shinshu University, Wakasato, Nagano 380-8553, Japan

[d]Present address: Nagano Prefectural Institute of Technology, Shimonogou, Ueda, Nagano 386-1211, Japan

Abstract

Semiconducting single-walled carbon nanotubes (SWNTs) have been enriched by 1-aminopyrene treatment of the mildly oxidized SWNTs due to removal of metallic SWNTs having a higher affinity for 1-aminopyrene. The enrichment was caused by the differences in the adsorption properties of 1-aminopyrene on the metallic and semiconducting SWNTs. The fluorescence properties of 1-aminopyrene adsorbed on the metallic and semiconducting

SWNTs have been investigated in order to clarify its adsorption mechanism. 1-Aminopyrene was adsorbed on the metallic SWNTs through the interaction of the amino group with the graphene surface and through a hydrogen bonding interaction between the amino group and the carboxyl group on the graphene surface. On the other hand, in the case of semiconducting SWNTs, 1-aminopyrene was adsorbed through a π-π interaction on the graphene surface in addition to the hydrogen bonding interaction with the carboxyl groups.

Keywords: Fluorescence; 1-aminopyrene; Adsorption; Single-walled carbon nanotubes; Metallic carbon nanotubes; Semiconducting carbon nanotubes

*Corresponding author: Hiromasa Nishikiori

Tel.: +81-26-269-5536

Fax: +81-26-269-5550

E-mail address: nishiki@shinshu-u.ac.jp

1. Introduction

Single-walled carbon nanotubes (SWNTs) have received considerable research attention due to their many potential applications [1, 2]. The SWNTs contain both metallic and semiconducting SWNT species, which has prevented widespread acceptability. If metallic and semiconducting SWNTs can be separated, they can be individually applied to the development of nanometer-sized conductors and field-effect transistors, respectively [3, 4]. Therefore, many researchers have attempted to separate metallic and semiconducting SWNTs by using aliphatic amine adsorption, tetracarboxyl coronene adsorption, porphyrin adsorption, H_2O_2 treatment, agarose gel electrophoresis, and microwave radiation [5-11]. Aliphatic amine molecules are selectively adsorbed on metallic SWNTs through an interaction utilizing the amino group [12]. This selectivity is attributed to the higher density of state (DOS) of the metallic SWNTs at the Fermi level. The inverse phenomenon is often observed after acid-treatment of SWNTs [13]. This phenomenon is attributed to quicker charge transfers from the amino group of the amine to the SWNT hole-doped by the acid treatment. Furthermore, the oxidation level of the SWNTs is an important factor in the selectivity of the amine adsorption [13, 14].

In this paper, we report the fluorescence properties of an aromatic amine, 1-aminopyrene, adsorbed on metallic and semiconducting SWNTs. The aromatic amine is expected to be adsorbed on the oxidized surfaces of the SWNTs in three ways [5, 12]. On the graphene

surface, the aromatic amine is adsorbed through a π-π interaction (aromatic ring) or an interaction utilizing the amino group (N lone pair or H atom of NH_2). On the other hand, the aromatic amine is also adsorbed through a hydrogen bonding interaction with the carboxyl groups on the SWNTs [15]. The adsorption properties of the aromatic amine can be expected to differ between metallic and semiconducting SWNTs depending on their DOS. Therefore, we attempted to enrich metallic or semiconducting SWNTs by using 1-aminopyrene and taking advantage of the differences in the adsorption properties. The fluorescence properties of 1-aminopyrene adsorbed on the metallic and semiconducting SWNTs were investigated in order to clarify its adsorption mechanism. The adsorbed 1-aminopyrene can be desorbed by dispersing the SWNTs into some concentration of acid solution due to their positive electrostatic repulsion.

2. Experimental

2.1. Enrichment of metallic or semiconducting SWNTs

The SWNTs (HiPco, carbon nanotechnologies) were added to a mixture of concentrated nitric acid and sulfuric acid (v:v = 1:3) and then mildly sonicated for 30 min. This sample was designated as Ac-SWNT. Oxygen-containing groups were produced by the oxidation of the SWNT surface in order to enhance the dispersibility of the SWNTs and their interaction with 1-aminopyrene in solvents. Thirty milligram of this Ac-SWNT and 0.1 g of

1-aminopyrene were added to 20 cm^3 of anhydrous tetrahydrofuran (THF) and then refluxed for 48 h at 340 K in order to adsorb 1-aminopyrene on the Ac-SWNT. The suspension was filtered with suction using a membrane filter with 0.1 μm pore size (Advantec H010A047A) in order to remove the highly dispersed SWNTs adsorbing a large amount of 1-aminopyrene. The resultant solid was designated as Ap-SWNT. Raman spectra of the Ac-SWNT and Ap-SWNT were obtained with a Jasco NRS-2100 spectrophotometer using laser excitation at 633 nm to determine their metallic and semiconducting characteristics. Raman spectra of the SWNTs contained in the filtrate of the suspension could not be observed because their amount was too small to detect a valid signal.

2.2. Fluorescence measurements

The adsorption properties of 1-aminopyrene on metallic and semiconducting SWNT surfaces were investigated by the fluorescence measurements. However, the fluorescence of the aromatic molecules adsorbed on the SWNT aggregates was scarcely observed due to strong quenching. Our unique procedure to create a highly dispersed system of individual SWNTs throughout solvents allowed the fluorescence observations. Either the Ac-SWNT or Ap-SWNT (0.20 mg) was individually dispersed in a 1-aminopyrene aqueous solution (10 cm^3) with a molar concentration of 1.0×10^{-4} or 1.0×10^{-5} mol dm^{-3} by ultrasonic irradiation in order to adsorb 1-aminopyrene on each SWNT. The resulting suspensions were centrifuged to remove any precipitates for fluorescence measurements because the SWNT

aggregates cause quenching of 1-aminopyrene in water. The fluorescence and fluorescence excitation spectra of the resulting supernatant suspensions were then measured using a Shimadzu RF-5300 spectrofluorophotometer. The suspension sample contained the 1-aminopyrene molecules in the liquid phase, which were not removed in this study because the spectra of the 1-aminopyrene molecules on the SWNTs and in the solution are distinguished by their characteristic shapes and peak positions [15].

3. Results and discussion

3.1. Characterization of Ac-SWNT and Ap-SWNT by Raman spectroscopy

Raman spectra of the untreated SWNT, Ac-SWNT, and Ap-SWNT were obtained in order to estimate the relative amounts of the metallic and semiconducting SWNTs in each SWNT sample. Figures 1 and 2 shows the Raman spectra of the SWNT and Ac-SWNT obtained upon the 633 nm laser excitation. The assignment of their metallic and semiconducting bands was carried out using a Kataura plot. Figure 1 (a) shows the radial breathing modes (RBM) of the SWNT (dotted line) and Ac-SWNT (solid line) in the 150 – 300 cm^{-1} region. The RBM spectrum is separated into two resonances— the resonance of the metallic (M_{11}) band (200 and 221cm^{-1}) and the semiconducting (S_{22}) band (258 cm^{-1}). The relative intensity of the M_{11} band in the Ac-SWNT was higher than that in the SWNT. As already known, the acid treatment selectively oxidized the semiconducting SWNTs and increased the

metallic SWNTs [9]. The M_{11} band of Ac-SWNT exhibited a larger Raman shift than that of the SWNT, indicating that the Ac-SWNT contained small diameter metallic SWNTs [16, 17]. This is because the large diameter metallic SWNTs were violently oxidized due to their high density of state at the Fermi level and removed by the filtration [18]. On the other hand, the semiconducting SWNTs were well oxidized and removed, regardless of their diameter, due to their high reactivity. Figure 1 (b) shows the G-band of the SWNT (dotted line) and Ac-SWNT (solid line) in the 1500−1700 cm^{-1} region. The G-band of the semiconducting SWNTs consists of a strong band at around 1590 cm^{-1} and a weak band at around 1570 cm^{-1}. The G-band of the metallic SWNTs also shows a strong band at 1580−1590 cm^{-1} [5, 7]. In addition, the Breit-Wigner-Fano band which is one of the bands due to metallic SWNTs was observed at around 1550 cm^{-1} [7, 18]. This band is highly sensitive to the electronic effects. The acid treatment oxidized not only the semiconducting SWNTs, but also the metallic SWNTs. Only the Breit-Wigner-Fano band disappeared after the acid treatment due to lowering the Fermi level by the oxidation of the SWNT surface [7]. The decrease in this band intensity does not indicate the decrease in the metallic SWNTs.

(Figure 1)

Figure 2 (a) shows the RBM of the Ac-SWNT (solid line) and Ap-SWNT (broken line) in the 150 - 300 cm^{-1} region. The relative intensity of the S_{22} band in the Ap-SWNT was higher than that in the Ac-SWNT. As the percentages of the metallic and semiconducting

SWNTs are regarded as 27% and 73% for SWNT according to the reference values [19], those can be estimated to be 36% and 64% for Ac-SWNT and 27% and 73% for Ap-SWNT from the relative intensities of the M_{11} and S_{22} bands, respectively. The S_{22} band of Ap-SWNT exhibited a larger Raman shift than that of the Ac-SWNT because the Ap-SWNT contained small diameter semiconductor SWNTs [16, 17]. The large diameter SWNTs were removed by filtration. This reason is discussed in Section 3.3.

Figure 2 (b) shows the G-band of the Ac-SWNT (solid line) and Ap-SWNT (broken line) in the 1500 – 1700 cm^{-1} region. The relative intensity of the band at around 1570 cm^{-1} in the Ap-SWNT was higher than that in the Ac-SWNT. This band originates from the semiconducting SWNTs [5, 7]. These results indicate that the semiconducting SWNTs were enriched in the Ap-SWNT compared to that in the Ac-SWNT. Therefore, the filtrate of the Ac-SWNT dispersion in THF contains concentrated metallic SWNTs. Maeda et al. have reported selective interactions between the amino group of aliphatic amines and the graphene sheet of air-oxidized metallic SWNTs (oxidation at lower levels) [14]. Therefore, our results suggest that the interaction between the amino group of 1-aminopyrene and the graphene sheet of the metallic SWNTs is stronger due to the mild oxidation of the SWNTs used in our experiment. However, the adsorption through a π-π interaction is also considerable because 1-aminopyrene has an aromatic ring. In order to clarify the adsorption properties of 1-aminopyrene on each SWNT, fluorescence measurements of

1-aminopyrene adsorbed on the SWNTs is essential.

(Figure 2)

3.2. Fluorescence properties of 1-aminopyrene adsorbed on SWNTs

1-Aminopyrene is a useful fluorescence probe for studying the physicochemical properties of the surrounding environment because it emits original fluorescences depending on the surrounding environment [15]. Figure 3 shows the fluorescence and fluorescence excitation spectra of 1-aminopyrene in various solvents. 1-Aminopyrene in water exhibits a broad fluorescence band at 440 nm, while the peaks of its fluorescence excitation are located at 357 and 388 nm. On the other hand, 1-aminopyrene in hydrochloric acid (5 mol dm^{-3}) exhibits vibronic bands at around 370–400 nm in the fluorescence spectrum, and the peaks are at 325 and 340 nm in the fluorescence excitation spectrum. The proton dissociation equilibrium constant of the ground state (pK_a) and the excited state (pK_a^*) are 2.8 and -1.2, respectively [20]. Therefore, the 1-aminopyrene bands in water and hydrochloric acid can be assigned to the neutral species (AP) and the protonated species (APH^+), respectively. 1-Aminopyrene in cyclohexane exhibits fluorescence peaks at 400 and 420 nm and fluorescence excitation peaks at 360 and 375 nm. The 1-aminopyene fluorescence in cyclohexane has a blue shift compared to that in water; this indicates that the structural relaxation of 1-aminopyene in cyclohexane in excited states is smaller than that in water.

(Figure 3)

Figure 4 shows the fluorescence and fluorescence excitation spectra of 1-aminopyrene in the aqueous dispersions of SWNTs and in cycolohexane. 1-Aminopyrene in the Ac-SWNT aqueous dispersion exhibited vibronic bands at around 370–400 nm in the fluorescence spectrum, while the peaks were present at 325 and 340 nm in the fluorescence excitation spectrum. These spectra are similar to those of APH^+. This indicates that 1-aminopyrene forms the APH^+-like species by hydrogen bonding between its amino group and carboxyl group on the Ac-SWNT surface [15].

The fluorescence of 1-aminopyrene in the Ap-SWNT aqueous dispersion exhibited peaks at 400 and 420 nm in addition to vibronic bands at around 370–400 nm due to APH^+-like species. In the fluorescence excitation spectrum, peaks at 357 and 374 nm appeared in addition to the APH^+-like peak at 340 nm. The peaks at 400 and 420 nm in the fluorescence and at 357 and 374 nm in the fluorescence excitation nearly correspond to those of 1-aminopyrene in cyclohexane. We have previously shown that 1-naphthol and pyrene were adsorbed on carbon nanotubes through a π-π interaction by observing fluorescences that were similar to those in non-polar solvents such as cyclohexane [21-23]. Therefore, by applying the same reasoning, these peaks can be attributed to the adsorption of 1-aminopyrene through the π-π interaction onto the graphene sheet of the SWNTs. In short, the fluorescence measurement revealed that 1-aminopyrene formed the APH^+-like species by hydrogen bonding with the carboxyl group on both the Ac-SWNT and Ap-SWNT and formed

the π-stacking species on only the Ap-SWNT containing a larger amount of the semiconducting SWNTs.

(Figure 4)

3.3. Adsorption mechanism of 1-aminopyrene on the SWNTs

Based on the results of the Raman spectra, it was found that the semiconducting SWNTs are enriched in the Ap-SWNT compared to that in the Ac-SWNT. This indicates that the metallic SWNTs were removed from the Ac-SWNT by amine treatment due to their higher affinity for 1-aminopyrene. On the air-oxidized metallic SWNTs (oxidation at lower levels), the amino groups of aliphatic amines selectively interact with the graphene sheet of the metallic SWNTs [13]. Therefore, it is suggested that 1-aminopyrene is adsorbed on the graphene surface of the metallic SWNTs through the interaction of the amino group (N lone pair or H atom of NH_2) in addition to the hydrogen bonding interaction [5, 6]. The quenching at a close distance between 1-aminopyrene and the SWNTs is the reason we cannot observe the fluorescence of the interaction specie by the amino group. A larger amount of 1-aminopyrene molecules was adsorbed on the graphene surface of the Ac-SWNT containing a larger amount of the metallic SWNTs though the interaction of the amino group. Therefore, 1-aminopyrene cannot be adsorbed on the graphene sheet of the Ac-SWNT through a π-π interaction.

Based on these results, an adsorption model of 1-aminopyrene adsorbed on the SWNTs is

proposed in Figure 5. As shown in Fig.5 (a), 1-aminopyrene is adsorbed on the metallic SWNTs through the interaction with the amino group on the graphene surface and through the hydrogen bonding interaction with the carboxyl group. On the other hand, 1-aminopyrene is adsorbed on the semiconducting SWNTs through the π-π interaction on the graphene surface and through the hydrogen bonding interaction with the carboxyl groups, as shown in Fig. 5 (b). Thus, the difference in the adsorption mechanism on each SWNT allows recognition of metallic SWNT and semiconducting SWNT. The larger diameter semiconductor SWNTs have a higher planarity and adsorbed a larger amount of 1-aminopyrene through π-π interaction. Therefore, parts of the larger diameter semiconductor SWNTs were better dispersed in the solvent and removed by filtration, causing the larger S_{22} band shift as shown in Fig. 2(a).

(Figure 5)

4. Conclusion

Metallic SWNTs were removed from the mildly oxidized SWNTs (Ac-SWNT) by 1-aminopyrene treatment due to their higher affinity for 1-aminopyrene, and consequently, semiconducting SWNTs were enriched in the residual SWNTs (Ap-SWNT). This is attributed to the stronger interaction between 1-aminopyrene and the metallic SWNTs. The adsorption mechanism was clarified by observing the fluorescence spectra of 1-aminopyrene

adsorbed on the SWNTs. Based on the results, it was concluded that the enrichment is caused by differences in the adsorption properties of 1-aminopyrene on the metallic and semiconducting SWNTs. In the case of metallic SWNTs, 1-aminopyrene was adsorbed through the interaction of the amino group with the graphene surface and through the hydrogen bonding interaction between the amino group and the carboxyl group on the graphene surface. On the other hand, in the case of semiconducting SWNTs, 1-aminopyrene was adsorbed through the π-π interaction on the graphene surface in addition to the interaction with the carboxyl group. These results are attributed to the difference in the density of state at the Fermi level between the metallic and semiconducting SWNTs.

Acknowledgements

This research was supported by CLUSTER (the second stage) and a Grant-in-Aid for Scientific Research (No. 21915015) from the Ministry of Education, Culture, Sports Science and Technology, Japan.

References

[1] S.J. Tans, M.H. Devoret, H. Dai, A. Thess, R.E. Smalley, L.J. Geerligs, C. Dekker, Nature 386 (1997) 474.

[2] R. Zeineldin, M. Al-Haik, L. G. Hudson, Nano. Lett. 9 (2009) 751.

[3] Z. Yao, C.L. Kane, C. Dekker, Phys. Rev. Lett. 84 (2000) 2941.

[4] S.J. Tans, A.R.M Verschueren, C. Dekker, Nature 393 (1998) 49.

[5] D. Chattopadhyay, I. Galeska, F. Papadimitrakopoulos, J. Am. Chem. Soc. 125 (2003) 3370.

[6] S.Y. Ju, M. Utz, F. Papadimitrakopoulos, J. Am. Chem. Soc. 131 (2009) 6775.

[7] R. Voggu, K.V. Rao, S.J. George, C.N.R Rao, J. Am. Chem. Soc. 132 (2010) 5560.

[8] H. Li, B. Zhou, Y. Lin, L. Gu, W. Wang, K.A.S. Fernando, S. Kumar, L.F. Allard, Y.P. Sun, J. Am. Chem. Soc. 126 (2004) 1014

[9] Y. Miyata, Y. Maniwa, H. Kataura, J. Phys. Chem. B 110 (2006) 25.

[10] T. Tanaka, H. Jin, Y. Miyata, H. Kataura, App. Phys. Exp. 1 (2008) 114001

[11] J.W. Song, H.W. Seo, J.K. Park, J.E. Kim, D.G. Choi, C.S. Han, Curr. Appl. Phys. 8 (2008) 725.

[12] Y. Maeda, S. Kimura, M. Kanda, Y. Hirashima, T. Hasegawa, T. Wakahara, Y. Lian, T. Nakahodo, T. Tsuchiya, T. Akasawa, J. Liu, X. Zhang, Z. Gao, Y. Yu, S. Nagase, S. Kazaoui, N. Minami, T. Shimizu, H. Tokumoto, R. Saito, J. Am. Chem. Soc. 127 (2005) 10287.

[13] J. Lu, L. Lai, G. Luo, J. Zhou, R. Qin, D. Wang, Lu Wang, W.N. Mei, G. Li, Z. Gao, S. Nagase, Y. Maeda, T. Akasaka, D. Yu, Small, 3 (2007) 1566.

[14] Y. Maeda, Y. Takano, A. Sagara, M. Hashimoto, M. Kanda, S. Kimura, Y. Lian, T. Nakahodo, T. Tsuchiya, T. Wakahara, T. Hasegawa, S. Kazaoui, N. Minami, J. Liu, S. Nagase, Carbon 46 (2008) 1563.

[15] H. Nishikiori, N. Tanaka, T. Tanigaki, M. Endo, T. Fujii, J. Photochem. Photobiol. A: Chem. 193 (2008) 161.

[16] A. M. Rao, J. Chen, E. Richter, U. Schlecht, P. C. Eklund, R. C. Haddon, U. D. Venkateswaran, Y.-K. Kwon, D. Tománek, Phys. Rev. Lett. 86 (2001) 3895.

[17] D. Chattopadhyay, I. Galeska, F. Papadimitrakopoulos, J. Am. Chem. Soc. 125 (2003) 3370.

[18] S. Kubota, D. Shimamoto, J. S. Park, H. Nishikiori, N. Tanaka, Y. A. Kim, T. Fujii, M. Endo, M. S. Dresselhaus, Chem. Commun. 46 (2010) 6977.

[19] Y. Miyata, K. Yanagi, Y. Maniwa, H. Kataura, J. Phys. Chem. C 112 (2008) 13187.

[20] H. Shizuka, K. Tsutsumi, H. Takeuchi, I. Tanaka, Chem. Phys. Lett. 62 (1979) 408.

[21] H. Nishikiori, N. Tanaka, S. Kubota, M. Endo, T. Fujii, Chem. Phys. Lett. 390 (2004) 389.

[22] S. Kubota, H. Nishikiori, N. Tanaka, M. Endo, T. Fujii, Chem. Phys. Lett. 412 (2005) 223.

[23] T. Tanigaki, H. Nishikiori, S. Kubota, N. Tanaka, M. Endo, T. Fujii, Chem. Phys. Lett. 448 (2007) 218.

Figure captions

Figure 1

(a) Radial breathing mode (RBM) and (b) G-band in Raman spectra of SWNT (dotted line) and Ac-SWNT (solid line) obtained with 633-nm laser excitation. The spectra are normalized at each peak intensity.

Figure 2

(a) Radial breathing mode (RBM) and (b) G-band in Raman spectra of Ac-SWNT (solid line) and Ap-SWNT (broken line) obtained with 633-nm laser excitation. The spectra are normalized at each peak intensity.

Figure 3

(a) Fluorescence and (b) fluorescence excitation spectra of 1-aminopyrene in (1) water, (2) hydrochloric acid (5 mol dm^{-3}), and (3) cyclohexane. (a) Excitation wavelength was 335 nm, and (b) Emission wavelengths were (1) 460 nm, (2) 375 nm, and (3) 405 nm. The spectra are normalized at each peak intensity.

Figure 4

(a) Fluorescence and (b) fluorescence excitation spectra of 1-aminopyrene in (1) Ac-SWNT aqueous dispersion, (2) Ap-SWNT aqueous dispersion, and (3) cyclohexane without SWNTs. (a) Excitation wavelength was 335 nm, and (b) Emission wavelengths were (1 and 2) 460 nm, and (3) 405 nm. The spectra are normalized at each peak intensity.

Figure 5

Pictorial representation of the proposed model of 1-aminopyrene adsorption on (a) metallic SWNTs and (b) semiconducting SWNTs.

Figure 1

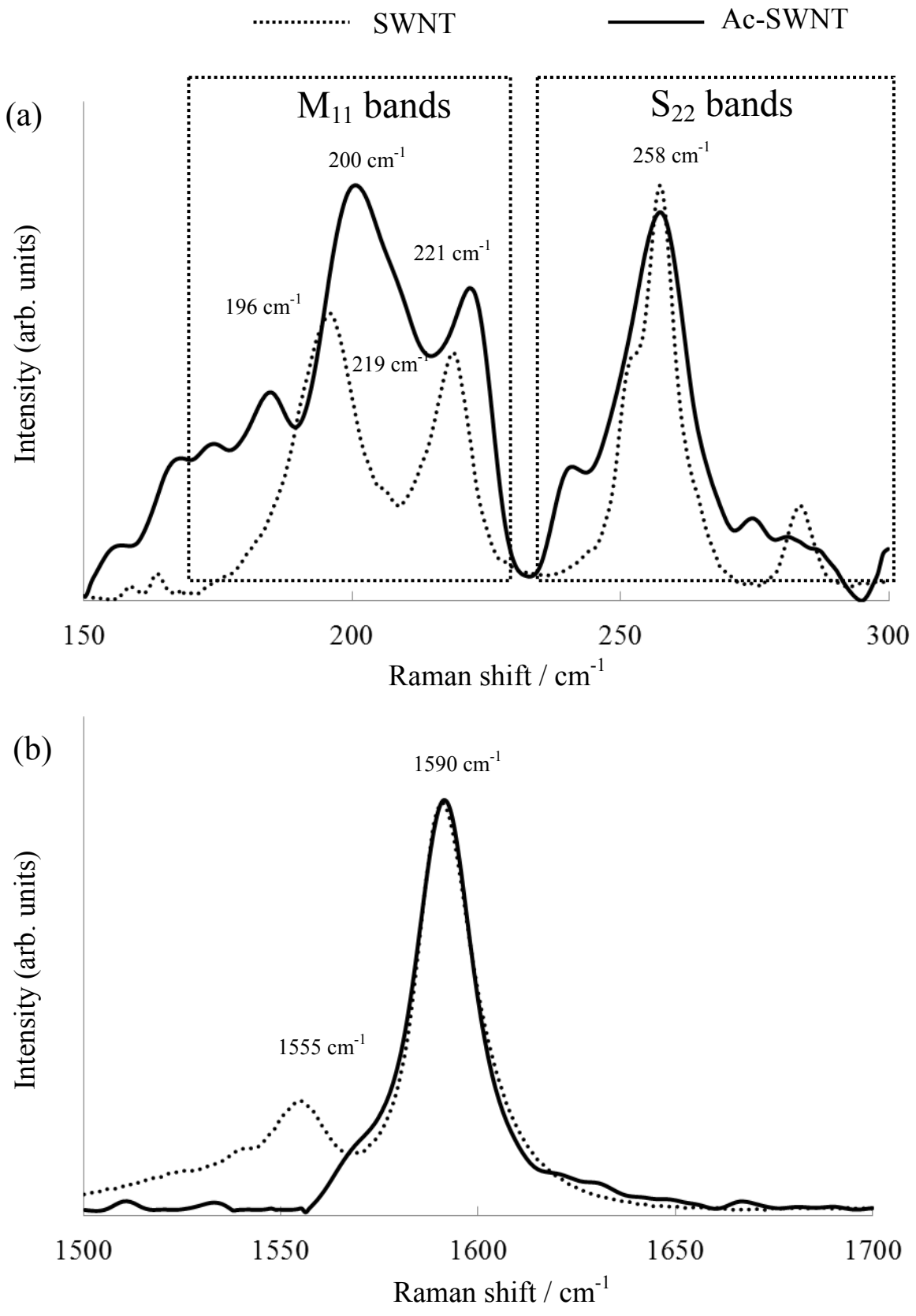
SWNT
Ac-SWNT
(a)
M_{11} bands
S_{22} bands
200 cm-1
258 cm-1
221 cm-1
196 cm-1
219 cm-1
Intensity (arb. units)
150
200
250
300
Raman shift / cm-1
(b)
1590 cm-1
1555 cm-1
Intensity (arb. units)
1500
1550
1600
1650
1700
Raman shift / cm-1

Figure 2

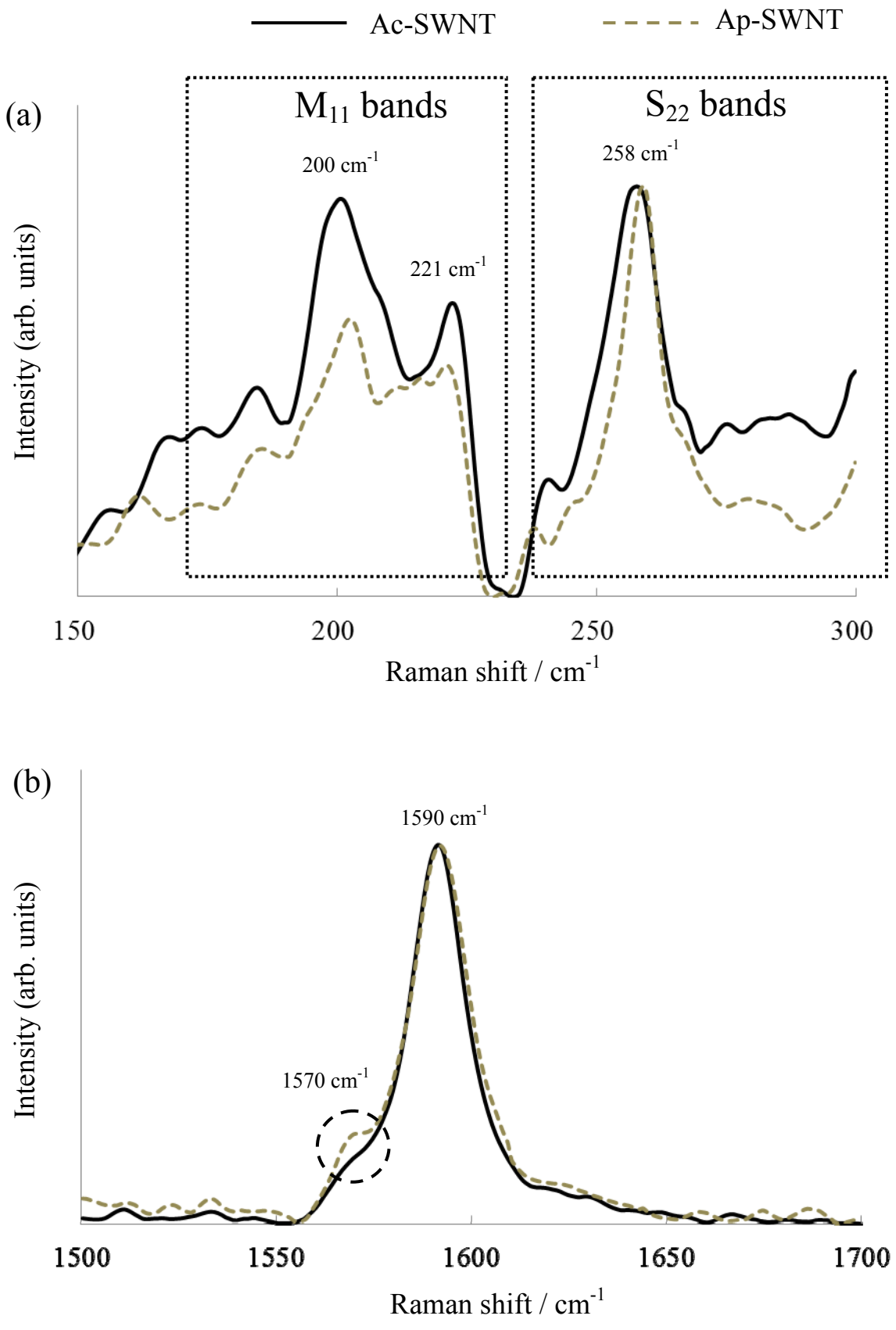
Ac-SWNT
Ap-SWNT
(a)
M11 bands
S22 bands
200 cm-1
221 cm-1
258 cm-1
Intensity (arb. units)
150
200
250
300
Raman shift / cm-1
(b)
1590 cm-1
1570 cm-1
Intensity (arb. units)
1500
1550
1600
1650
1700
Raman shift / cm-1

Figure 3

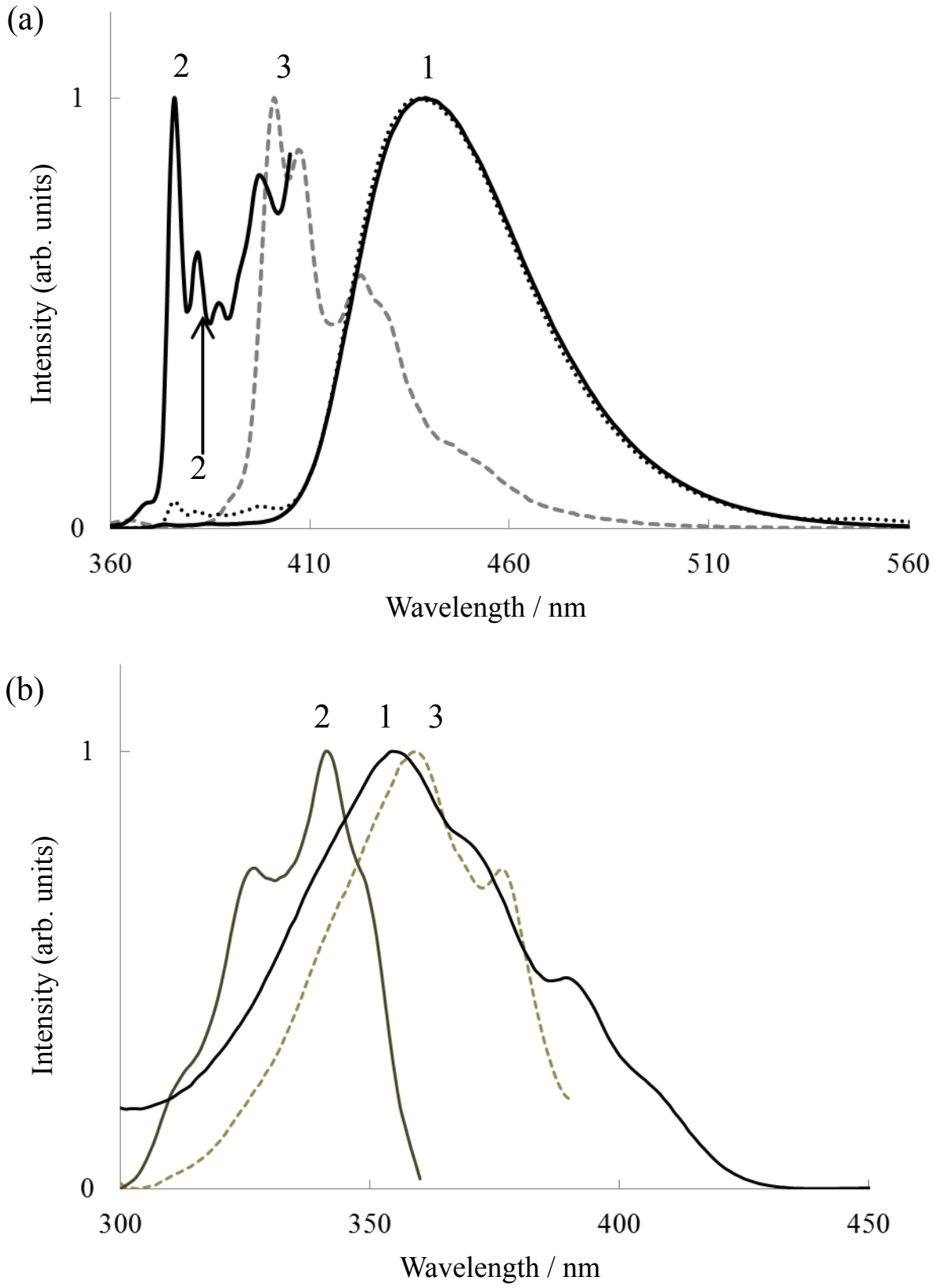
(a)
2
3
1
1
0
Intensity (arb. units)
2
360
410
460
510
560
Wavelength / nm
(b)
2
1
3
1
0
Intensity (arb. units)
300
350
400
450
Wavelength / nm

Figure 4

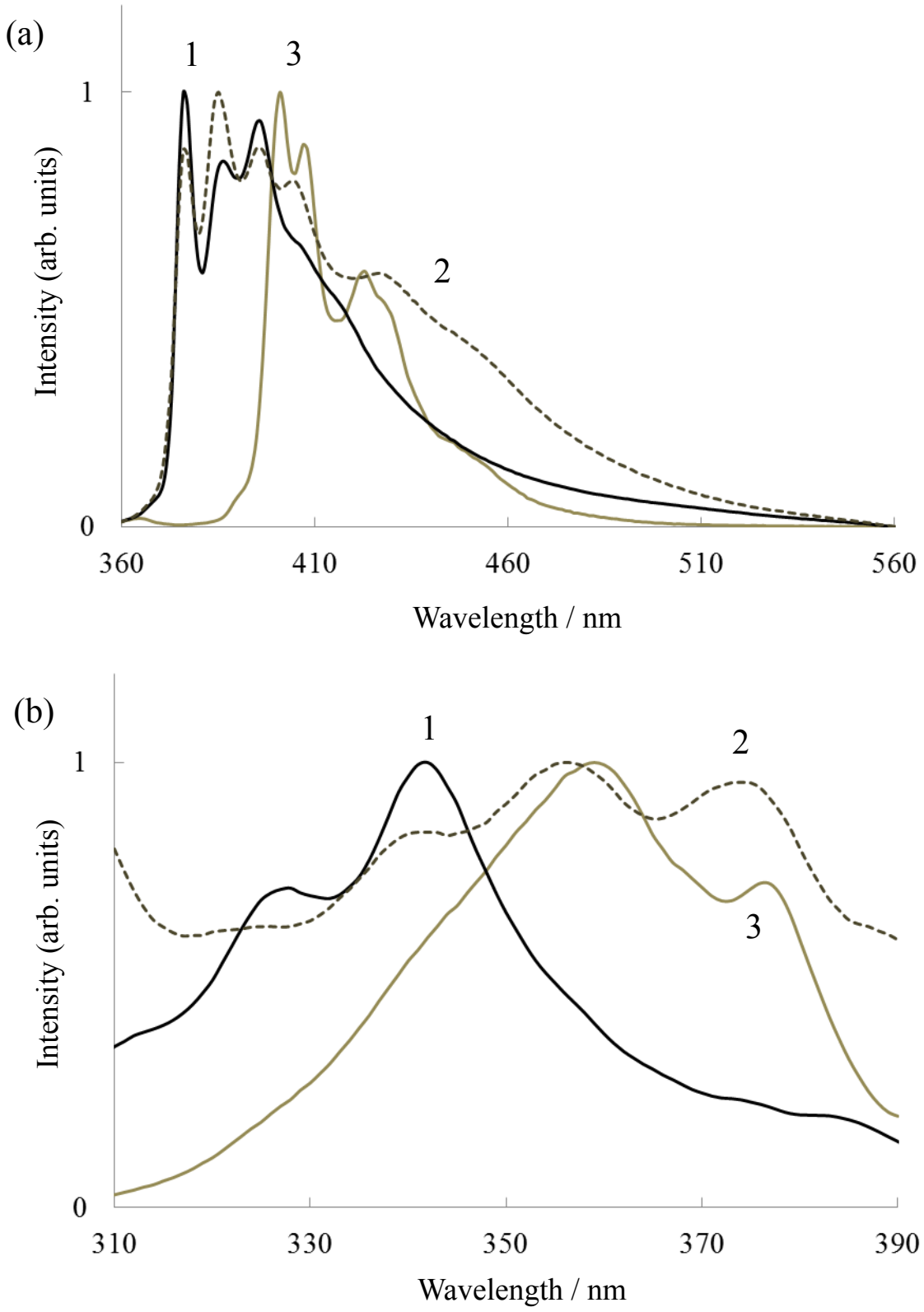
(a)
1
3
2
1
0
Intensity (arb. units)
360
410
460
510
560
Wavelength / nm
(b)
1
2
3
1
0
Intensity (arb. units)
310
330
350
370
390
Wavelength / nm

Figure 5

(a)

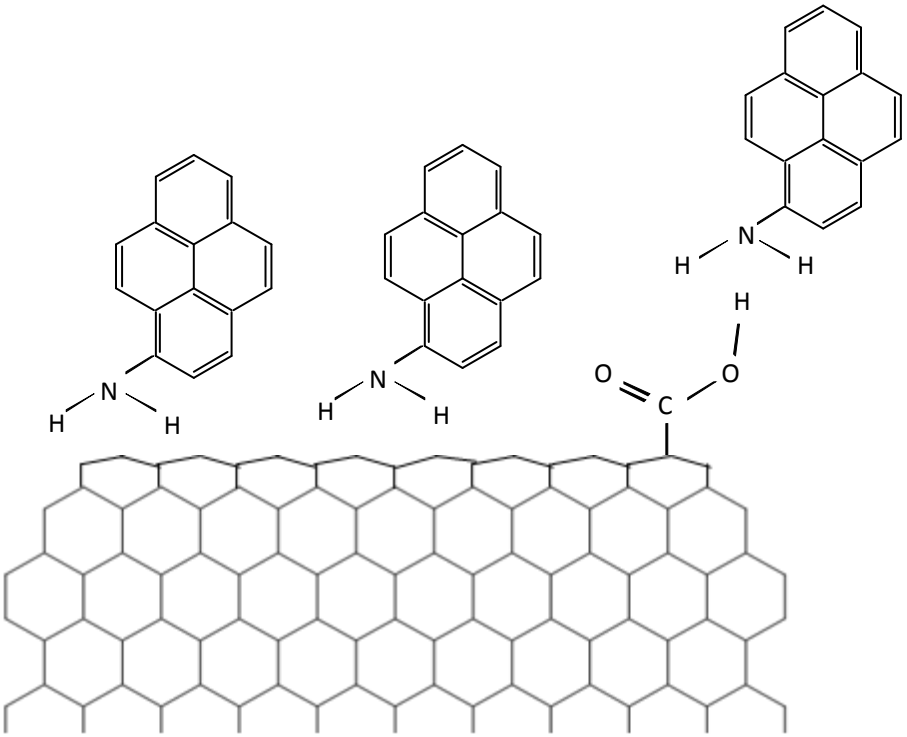

(b)